ATMOSPHERIC STRUCTURE OF THE OUTER PLANETS FROM THERMAL EMISSION DATA

Glenn S. Orton
Jet Propulsion Laboratory
California Institute of Technology
Pasadena, California 91103

ABSTRACT

Determination of atmospheric temperature structure is of paramount importance to the understanding of planetary atmospheric structure. The most powerful methods for determining atmospheric structure exploit the opacities provided by the collision induced H_2 dipole and the ν_4 fundamental of CH_4. In addition to earth-based observations, useful measurements of thermal emission from Jupiter and Saturn have been or soon will be made by several spacecraft, with results cross-checked with independent radio occultation results. For Uranus and Neptune, only a limited set of whole-disk earth-based data exists. All the outer planets show evidence for stratospheric temperature inversions; temperature minima range from about 105 K for Jupiter and 87 K for Saturn, to roughly 55 K for Uranus and Neptune. In addition to better data, remaining problems may be resolved by better quantitative understanding of gas and aerosol absorption and scattering properties, chemical composition, and non-LTE source functions. Ultimately, temperature structure results must be supplemented by quantitative energy equilibrium models which will allow some meaning to be given to the relationships between such characteristics as temperature, clouds, incident solar and planetary radiation, and chemical composition.

1. INTRODUCTION

Direct information about the structure of planetary atmospheres has been obtained through in situ probes for the earth, Mars and Venus. While the Galileo mission will investigate the Jovian atmosphere by a direct probe in the 1980's, current information on the structure of atmospheres in the outer solar system comes only from remote measurements. For this reason, the review presented here will be concerned with the large outer planets only, ignoring satellites with atmospheres for convenience alone.

Atmospheric structure, in the most general sense, includes consideration of vertical and horizontal variations of temperature, gaseous constituents, aerosols, and winds. For the outer planets, aerosol and wind structure are poorly understood. Chemical composition is reviewed by Encrenaz

C. G. Wynn-Williams and D. P. Cruikshank (eds.), Infrared Astronomy, 35–56.

and Combes in this volume. This review will concentrate on temperature structure. Information about temperature structure is very important for several reasons: (1) definition of basic structure by discrimination between regions dominated by radiative vs. convective energy transport, (2) interpretation of thermal emission to determine properties of gases and aerosols, (3) accurate interpretation and modelling of temperature-dependent physical processes, (4) determination of the strength and direction of thermally driven winds, and (5) definition of boundary conditions for models of thermal history and of the planetary interior.

2. TECHNIQUES

Temperature structure information from *in situ* probes is costly and the information gathered is extremely localized. On the other hand, vertical resolution can surpass what is available from remote infrared measurements. Furthermore, simultaneous remote and direct measurements offer a means for calibrating information derived from remote measurements.

Other remote techniques rely on occultation of a radiation source by the planet to sound atmospheric properties. Occultation of spacecraft radio signals by Jupiter (Lindal et al., 1980) and Saturn (Kliore et al., 1980) have been used to determine temperature structure, as has the occultation of α Leonis by Jupiter observed in the ultraviolet (Atreya et al., 1980). Occultation techniques offer the advantage of better vertical resolution than available from infrared sounding. However, there are several disadvantages, besides the relative infrequency of the appropriate geometric conditions. Foremost among these are the poor horizontal resolution and the need to assume homogeneity of the atmospheric structure along all points of the ray path. Another disadvantage for the radio occultation technique, the requirement that composition be known, has been used, in concert with "simultaneous" infrared coverage, to determine the bulk compositions of Jupiter (Gautier et al., 1980) and Saturn (Kliore et al., 1980; Orton and Ingersoll, 1980).

Energy (i.e. radiative-convective) equilibrium models could also be considered a form of temperature sounding. Indeed, results from a variety of other techniques must be analyzed in the context of such models in order to facilitate quantitative physical interpretation. The disadvantages of such techniques lie in their heavy dependence on *a priori* assumptions about the deposition of solar energy, as well as their lack of direct constraint to the observations. This review will use the work of Appleby and Hogan (1980) for comparison with direct sounding results, as their models take advantage of the most recent available data base. Earlier classic work by Trafton (1967), as well as the work of Hogan et al. (1969), Wallace et al. (1974), Wallace (1975), Cess and Khetan (1973), Trafton and Stone (1974), Cess and Chen (1975), Tokunaga and Cess (1977), and Danielson (1977) should not go without mention, however.

Temperature sounding, the direct inversion of thermal emission measurements to determine temperature structure (also known as temperature recovery or temperature retrieval), is used quite successfully in terrestrial applications with data supplied by earth-orbiting satellites. The technique requires a vertical interval to be defined from which the radiation contributing to the available thermal emission data has originated. For a clear atmosphere of infinite depth, one is required to invert a set of measured intensities, $I(\mu,\nu)$ in

$$I(\mu,\nu) = \int_{x_{bottom}}^{x_{top}} B[\nu,T(x)] \frac{\partial\tau(x,\nu)}{\partial x} dx \quad (1)$$

to recover the temperature structure $T(x)$. In equation 1, ν is frequency, μ is emission angle cosine, B is the Planck brightness function, x is any independent vertical parameter (e.g. altitude or logarithm of pressure), and $\tau(x)$ is the transmission between x and x_{top}; x_{top} is sufficient to approximate conditions of clear space and x_{bottom} those of infinite depth. Measurements and inversions also make use of intensities with a filtered integration over some spectral interval $\Delta\nu$; in such a case the parameters in the integrand must be integrated over $\Delta\nu$ explicitly, although for $\Delta\nu$ sufficiently small, an average value of B may be used with explicit computation of τ averaged over $\Delta\nu$.

The kernel of equation 1, $\partial\tau/\partial x$, is known as the weighting function and it must be known a priori, implying that the abundance of some opaque chemical constituent must be known--preferably a uniformly mixed gas. The recovery is influenced by assumptions about boundary conditions (Orton, 1977), such as the temperature structure above and below the vertical interval where temperatures are being determined. Vertical resolution is limited by data noise and width of the weighting function (Conrath, 1972). For the outer planets, a resolution element is never better than half an atmospheric scale height. A substantial literature exists on numerical techniques for inverting equation 1 (e.g., Deepak, 1977). This author has used the techniques described by Chahine (1972, 1975) because of their simplicity and stability.

3. APPLICATION

For the outer planets, the most important source of atmospheric opacity in the far infrared is that provided by the collision induced dipole of H_2, due to its great abundance as an atmospheric constituent and its dominance of almost all the opacity for wavelengths longer than 14 μm ($\nu \leq 700$ cm^{-1}), from which most of the thermal flux from the outer planets originates. As a collision induced phenomenon, its absorption is proportional to the square of the pressure and its weighting functions are therefore quite narrow. Figure 1 demonstrates the pressure corresponding to the location of unit optical depth for the H_2 dipole as a function of frequency for the outer planets. The broad translational band at shortest frequencies and two broad rotational lines, S(0) and S(1),

https://doi.org/10.1017/S0074180900075124 Published online by Cambridge University Press

respectively centered at 370 and 600 cm^{-1}, can easily be seen. A further advantage of this opacity source is that the broad spectral features allow useful data to be sampled over relatively broad spectral bandpasses without a debilitating loss of vertical resolution. For the 100 - 600 cm^{-1} region the vertical coverage extends from approximately 700 to 50 mb. At lower frequencies, coverage can sometimes extend down to higher pressure regions before another opacity source such as NH_3 influences the atmospheric opacity; this, in fact, appears to be the case for Uranus and Neptune.

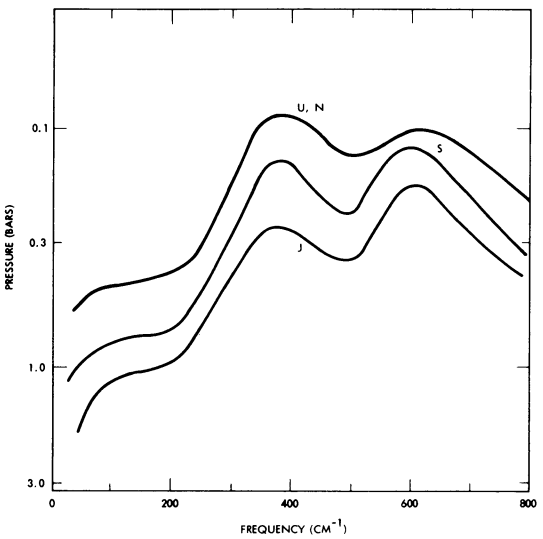

Figure 1. Pressure at which unit optical depth is reached in the atmospheres of the outer planets due to the opacity of the collision induced H_2 dipole, for a mixing ratio of 90%. Other opacity sources are not included.

There are problems involved with the use of the H_2 dipole opacity. The lowest temperature at which laboratory measurements of H_2 absorption have been made is 77 K (Birnbaum, 1978); more work must be done to understand the behavior of the absorption at lower temperatures (relevant to Uranus and Neptune). Furthermore, atmospheric models have thus far assumed a ratio of para-H_2 to ortho-H_2 which is always in equilibrium at the local temperature; this will not be true if the characteristic time scale for convection is faster than that for ortho-para conversion. Even if the correct ortho-H_2 to para-H_2 ratio were known everywhere, no models have been developed to express the opacity of different state ratios at all temperatures of interest. Finally, the broad features may be confused with other opacity sources, such as the distant wings of strong NH_3 rotational lines (near 100 cm^{-1}) or absorption by NH_3 ice particles. Figure 2 demonstrates the effect of an NH_3 ice haze in the atmosphere of Jupiter on the infrared spectrum. The effect is substantial, but for sufficiently large particle sizes, no distinctive spectral signature is

https://doi.org/10.1017/S0074180900075124 Published online by Cambridge University Press

seen. Approaches to this problem must involve simultaneous examination of several spectral regions where the particle optical properties differ substantially (e.g. in single scattering albedo), or simultaneous analysis of reflected solar radiation at shorter wavelengths.

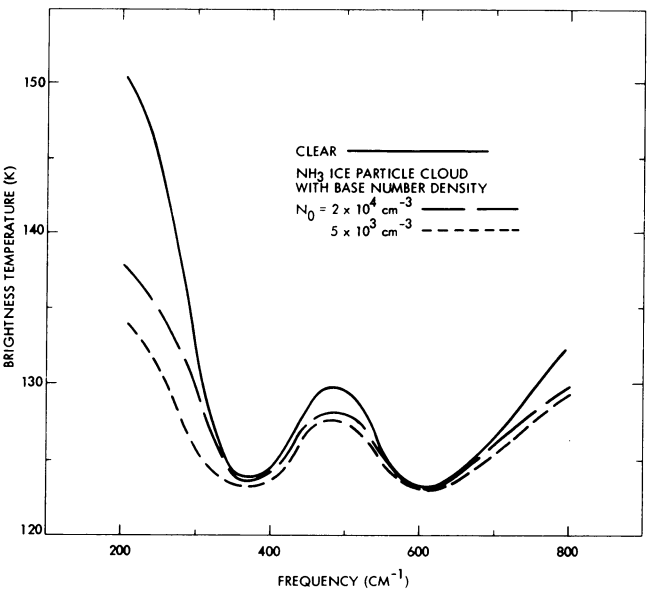

Figure 2. Effect of an NH_3 ice haze in the atmosphere of Jupiter on the thermal spectrum. The NH_3 particles are treated as spherical with a mode radius of 3 μm (and a 10% variance). The base of the cloud is at 670 mb (147 K) with the particle number density given, and the scale height is 20 times smaller than the gas scale height. (Note that the number density values are reversed.)

In order to extend vertical coverage to regions where the pressure is substantially less than 100 mb, where most of the outer planets have thermally inverted stratospheres, sufficient opacity is provided by the ν_4 fundamental band of CH_4 near 7.6 μm (1300 cm^{-1}). For Jupiter and Saturn, CH_4 is expected to be uniformly mixed throughout the atmosphere. Figure 3 shows the pressures associated with unit optical depth for Jupiter as a function of frequency in the region of the CH_4 ν_2 and ν_4 spectral region (for a spectral element with a full width at half maximum, FWHM, of 4 cm^{-1}, similar to that of the Voyager IRIS - Infrared Interferometer Spectrometer - experiment). Figure 4 displays sample weighting functions for both H_2 and CH_4 opacity dominated spectral regions. Weighting functions for CH_4 are somewhat dependent on spectral location and resolution, but they are at least twice as wide as for H_2 (except where the wing of an individual Lorentz line may be isolated).

https://doi.org/10.1017/S0074180900075124 Published online by Cambridge University Press

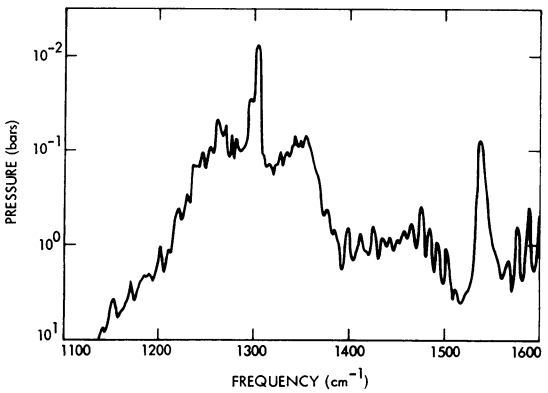

Figure 3. Pressure at which unit optical depth is reached in the atmosphere of Jupiter due to CH_4 opacity in the region of the ν_2 and ν_4 fundamentals. The FWHM of a resolution element is 4 cm^{-1} (from Orton and Robiette, 1980). The CH_4 mixing ratio is 1 x 10^{-3}.

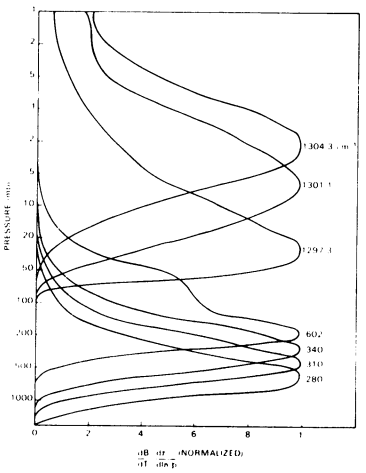

Figure 4. Weighting functions for H_2-dominated and CH_4-dominated regions of opacity in the Jovian spectrum (from Conrath and Gautier, 1980).

Temperature sounding with CH_4 has its own difficulties, beginning with the real problem of determining a good value for the atmospheric mixing ratio. Added to this is the disagreement among various laboratory studies on the absolute strength of ν_4 CH_4 lines, with an overall uncertainty still around 20% as of this writing (Orton and Robiette, 1980). Both Wallace and Smith (1976) and Orton (1977) have demonstrated the problem that thermal sounding at this frequency, where a small change in temperature produces a very large change in brightness, in the presence

https://doi.org/10.1017/S0074180900075124 Published online by Cambridge University Press

of a steep temperature gradient is poorly posed. A small change in the assumed temperature or non local thermodynamic equilibrium source function at very low pressures (but relatively high temperatures) may produce substantial changes in the temperatures recovered at higher pressures. Attempts to estimate the non-LTE source function are hampered by the lack of laboratory measurements of the ν_4 relaxation time constant under the influence of H_2 collisions in the relevant temperature range. In the atmospheres of Uranus and Neptune, CH_4 is expected to condense into the solid phase below the respective temperature minima, resulting in a non-uniform vertical distribution and an extremely small mixing ratio in the respective stratospheres. Finally, the ν_4 band is not located in a region of intrinsically high flux; thus, for the low temperatures of relevance, adequate signal is far more difficult to achieve than at longer wavelengths.

Other techniques could be used to extend the vertical sounding range. For example, extremely high resolution measurements of the ν_4 R(0) line could allow the weighting functions shown in Figure 5 to be formed. This could provide the opportunity to sound the stratosphere up to the level of 10^{-7} bars (although the problems associated with the non-LTE function and the extent to which the inversion is well-posed would still be present).

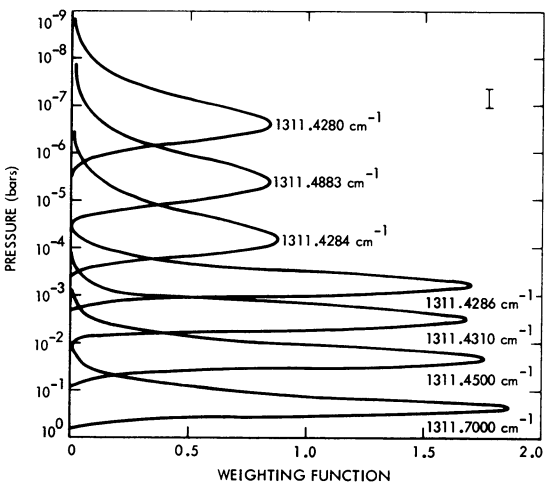

Figure 5. Weighting functions in the Jovian atmosphere, for the same model as in Fig. 3, for monochromatic radiation originating in the vicinity of the R(0) line at 1311.428 cm^{-1} (from Orton and Robiette, 1980).

To extend coverage deeper into the atmosphere, one possibility exists for Jupiter in which the "5-μm window", a spectral region (roughly 1900 - 2300 cm^{-1}) relatively free from strong gaseous absorption, could be used to sound by making use of the weak opacities associated with PH_3, NH_3 or CH_3D. However, not only is there a problem with determining

https://doi.org/10.1017/S0074180900075124 Published online by Cambridge University Press

the abundances of these constituents independently, but aerosol effects exert such a substantial influence that the region is best used for cloud and haze sounding. For Saturn and beyond, no substantial radiation is observed from this region, compared with that from Jupiter, and it is likely that a substantial fraction of radiation observed from those planets near 5 μm is, in fact, reflected sunlight. An alternative possibility for deeper atmospheric coverage is at very long wavelengths, where aerosol effects are minimized. Figure 6 illustrates the thermal emission spectra of the outer planets in this region. For Jupiter and Saturn, the gaseous opacity of NH_3 rotation-inversion lines would be useful for temperature sounding if the vertical distribution of NH_3 were well understood. For Uranus and Neptune, the long wavelength (low frequency) wing of the H_2 dipole translational band still dominates the opacity for wavelengths up to about 2 mm. It is a problem, however, to obtain useful spatially resolved data at such long wavelengths, even for spacecraft observations, as relatively large antennas are required to overcome diffraction limitations.

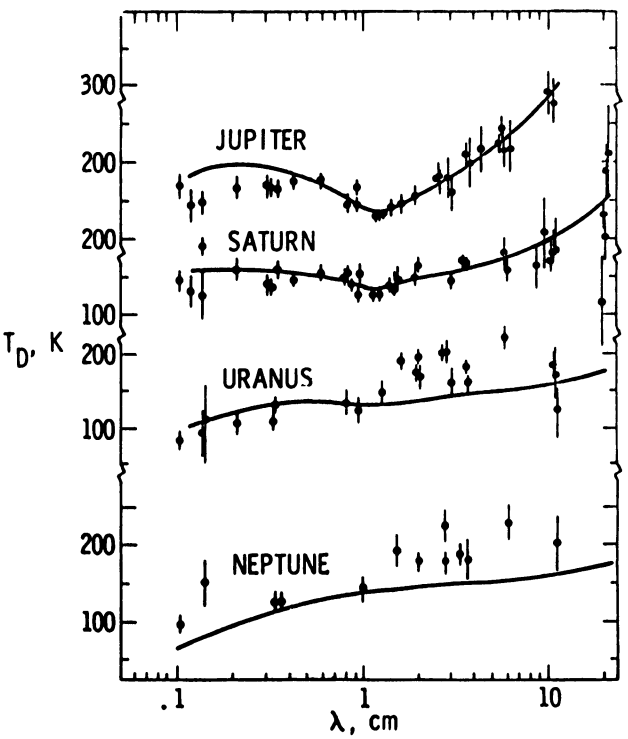

Figure 6. Composite microwave spectra of Jupiter (from Berge and Gulkis, 1976), Saturn (from Klein et al., 1978), Uranus (from Gulkis et al., 1978), and Neptune (from Gulkis and Olsen, 1980). Solid lines represent simple model spectra with H_2 and with NH_3 in saturation equilibrium.

https://doi.org/10.1017/S0074180900075124 Published online by Cambridge University Press

4. RESULTS

Jupiter

Early work on Jovian temperature sounding using earth-based data (Ohring, 1973; Orton, 1975b, 1977; Gautier et al., 1977a, 1979) and using Pioneer Infrared Radiometer results (Orton, 1975a; Orton and Ingersoll, 1976) has largely been superceded by the more recent and complete results of the Voyager IRIS experiment. Some of the first IRIS results (Hanel et al., 1979) are summarized in Figures 7 and 8.

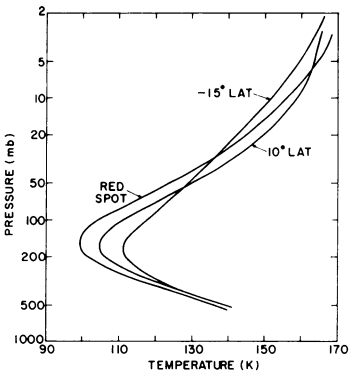

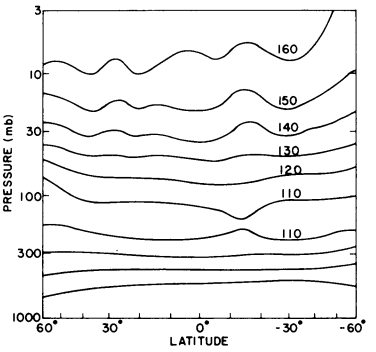

Figure 7. (Left) Examples of temperature profiles obtained by inversion of spectral radiances observed by the Voyager IRIS experiment (from Hanel et al., 1979). Figure 8. (Right) Zonally averaged meridional cross section of Jovian temperature structure recovered from Voyager IRIS experiment data (from Hanel et al., 1979).

One should note the relative steepness of the temperature structure both above and below the temperature minimum. Of further note are features which vary with position, such as the gradual increase in stratospheric temperatures from south to north, noted also in earth-based observations by Sinton et al. (1980). Presuming that the temperature inversions in the outer planets are due to thermalization of absorbed insolation, this temperature increase from south to north is most likely due to the slight tilt of the north pole of Jupiter sunward. Future monitoring of this feature with time as a function of changing insolation geometry will allow some conclusions to be drawn about the radiative relaxation time characterizing the Jovian stratosphere. It should also be noted that there is unexpected detail in the latitudinal structure of stratospheric temperatures, implying a non-uniform horizontal distribution of insolation-absorbing aerosols. One further feature of note (not illustrated in Figs. 7 or 8) is the strong drop (more than 5K) in temperatures over the Great Red Spot compared with the surrounding area near the 100 mb level. These may result from radiative equilibrium with reduced planetary flux emerging locally from below (Orton, 1975a) or from dynamical considerations (Flasar et al., 1980). It should be noted that analysis to date has not attempted to account systematically for the effects of

https://doi.org/10.1017/S0074180900075124 Published online by Cambridge University Press

(NH_3 ice) clouds around the 150 K level on outgoing emission. Latitudinal variations of temperatures recovered near 500 mb may therefore only reflect the variation of cloud thickness or cloud height from region to region.

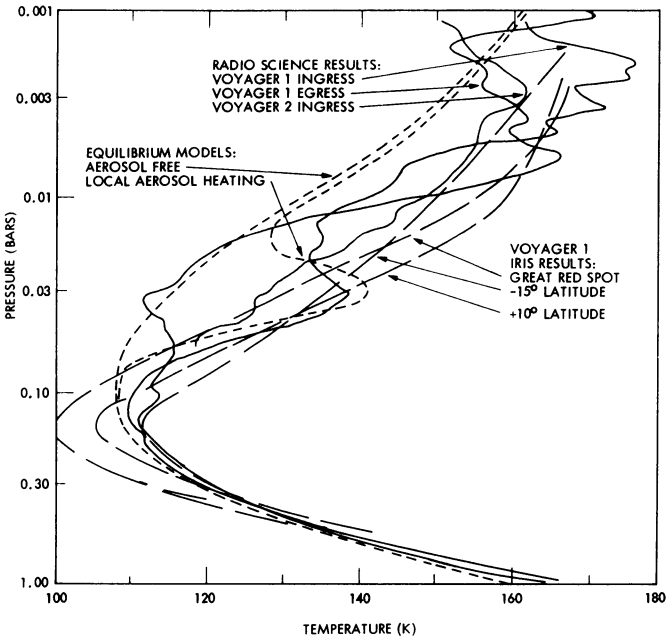

Figure 9. Comparison of Jovian temperature structures derived from Voyager radio occultation results (Lindal et al., 1980; solid line), IRIS results (Hanel et al., 1979; long dashed lines), and radiative-convective equilibrium models (Appleby and Hogan, 1980; short dashed lines). Equilibrium models are for a uniform distribution of insolation-absorbing aerosols and for a "local" distribution absorbing 4% of the total insolation.

Figure 9 demonstrates a visual comparison of the results of IRIS, the radio occultation results, and equilibrium models. The IRIS and radio occultation results are largely in agreement; for the tropopause and below the agreement has been optimized by an appropriate assumption for the bulk composition (Gautier et al., 1980). The radio results do, however, give an independent confirmation of the assumption of an adiabatic lapse rate for pressures near and greater than 1 bar. The detailed vertical structure of the occultation results are beyond the vertical resolution of infrared experiment retrieval. An unresolved question is whether the differences between the relatively cold Voyager 1 egress profile for the lower stratosphere and the relevant infrared data for this region are totally irreconcilable and whether the consistent difference in location of the temperature minimum is significant. The variable radio occultation results for the stratosphere are consistent

https://doi.org/10.1017/S0074180900075124 Published online by Cambridge University Press

with IRIS results implying a variation of insolation-absorbing aerosols with location of the planet. The Appleby and Hogan (1980) equilibrium models demonstrate that such an explanation is physically viable. The "cold" Voyager 1 occultation profile is never much lower than the thermal inversion supported by CH_4 absorption alone, whereas the Voyager 1 ingress profile vertical variation could easily be the result of heating by a "local" absorption of 4% of the total absorbed solar flux.

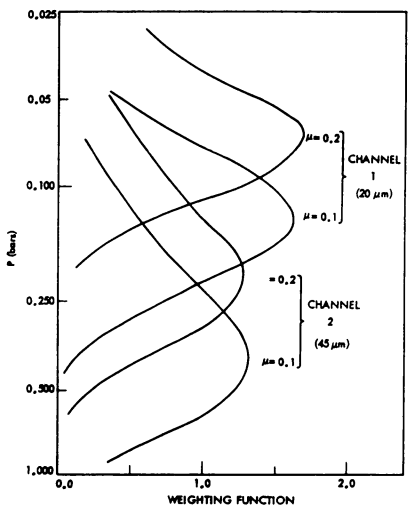

Figure 10. Weighting functions for the flux observed from Saturn in the two channels of the Pioneer 11 IRR (from Orton and Ingersoll, 1980). In this figure, μ is the emission angle cosine.

Saturn

Earth-based spectral observations formed the data base for early Saturn temperature sounding (Ohring, 1975; Gautier et al., 1977b) as well as semi-empirical radiative-convective equilibrium models by Tokunaga and Cess (1977). More recently, detailed information on Saturn has been obtained by the Pioneer 11 Infrared Radiometer in the same manner as the Pioneer 10 and 11 IRR data to determine the Jovian temperature structure (Orton, 1975a; Orton and Ingersoll, 1976). Weighting functions for the two broadband channels of the IRR, centered near 20 μm and 45 μm, are shown in Figure 10. Note that the weighting functions form a useful set only when a given area is observed over a range of emission angles. However, since the IRR observed no planetary position more than once, it was necessary to assume atmospheric longitudinal homogeneity. Figure 11 shows results for one of the warmest and one of the coolest regions observed. All models assume an adiabatic lapse rate below the 500 mb level and use a linear temperature interpolation in between the discrete levels where temperature is actually recovered. Cases 1 and 2 assume overlying inverted lapse rates consistent, respectively, with (1) the Pioneer 11 radio occultation results (Kliore et al., 1980) and (2) the

https://doi.org/10.1017/S0074180900075124 Published online by Cambridge University Press

equatorial model of Tokunaga and Cess (1977). Case 3 assumes that the apparently cooler temperatures at 500 mb near the equator are due to an unmodeled cloud influence. If the 500 mb temperatures are to be recovered with nearly equal values as for warmer poleward latitudes, the presence of a cloud must be invoked, modeled crudely as a uniform opaque blackbody surface emitting at approximately 124 K. If the cloud is composed of NH_3 ice particles, as is strongly suspected on Jupiter,

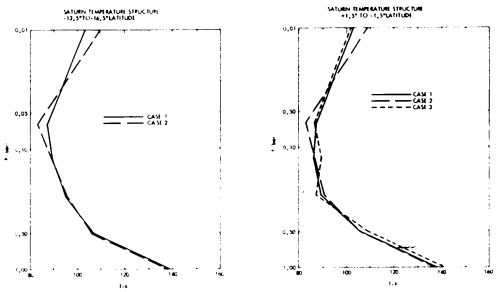

Figure 11. Temperatures recovered by the Pioneer 11 IRR for one of the warmest (left) and one of the coolest (right) regions observed (from Orton and Ingersoll, 1980).

it is substantially thicker on Saturn, since the cloud bottom is near the 150 K level. Figure 12 shows a smoothed plot of recovered temperatures vs. latitude for the region covered by IRR observations. Note that for all latitudes (and all cases) the temperature minimum region is substantially broader than for Jupiter (Figs. 7 and 8). The only major temperature variation with latitude, the cool equatorial (10°N to 10°S) region, correlates strongly with a region which is bright at visual wavelengths.

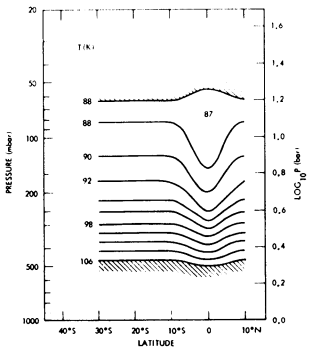

Figure 12. Smoothed contours of meridional cross section of Saturnian temperature structure for the region of the planet observed by the Pioneer 11 IRR (from Orton and Ingersoll, 1980).

https://doi.org/10.1017/S0074180900075124 Published online by Cambridge University Press

Figure 13 displays a comparison of Pioneer 11 IRR and radio occultation results with a radiative-convective equilibrium model (Appleby and Hogan, 1980). The models correspond reasonably well with one another below the temperature minimum, although the correlation between the infrared and radio occultation profiles has been optimized by an appropriate choice for the bulk composition (Kliore et al., 1980; Orton and Ingersoll, 1980). The temperature structures of Kliore et al. and those of Tokunaga and Cess (1977) above the temperature minimum are not reconcilable. In fact, the radio occultation temperatures fall below those of the equilibrium model.

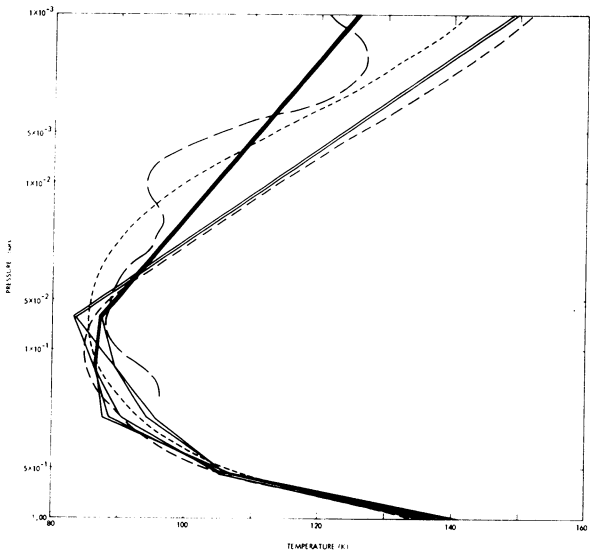

Figure 13. Comparison (from Orton and Ingersoll, 1980) of Saturnian temperature structures derived from Pioneer 11 IRR results for different regions and different assumptions (Orton and Ingersoll, 1980; solid lines), radio occultation results (Kliore et al., 1980; long dashed line), a model derived from earth-based data (Tokunaga and Cess, 1977; medium dashed line), and an equilibrium model (Appleby and Hogan, 1980; short dashed line). The equilibrium model has a uniform vertical distribution of aerosols.

Another noteworthy phenomenon is the substantial latitudinal dependence of the stratospheric temperatures observed from the earth, as illustrated in Figure 14. Elevated temperatures at the south pole are presumed to be due to the substantially greater amount of sunlight incident on the south pole at the time of the measurements. As for Jupiter, continued monitoring of the temperatures at both poles as the north goes into summer and the south into winter will provide useful information on the characteristic time constant for radiative thermal adjustment.

https://doi.org/10.1017/S0074180900075124 Published online by Cambridge University Press

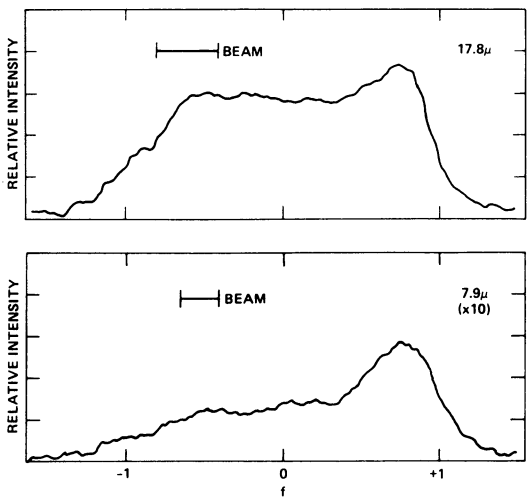

Figure 14. Spatially resolved meridional scans of Saturn obtained in March 1977, showing the south polar brightening in two spectral regions sensitive to stratospheric temperatures (from Tokunaga et al., 1978). Position on disk, relative to the polar radius, is given by f, with positive values to the south.

Finally, not only continued earth-based spatially resolved observations but also Voyager IRIS (and radio occultation) results should be able to resolve some of the questions raised by earlier results. Among these are the temperature structure of the stratosphere, the nature and distribution of NH_3 ice particles, the form of temperature or cloud asymmetries about the equator, and properties poleward of 30°S or 10°N.

Uranus and Neptune

The outermost known giant planets represent a whole separate class of observational problems involving dim objects for which no spatial resolution is available. Most of the thermal flux appears in a spectral region which is obscured from the ground by strong water vapor rotational line absorption. The inference from brightness temperature measurements and equilibrium models is that CH_4 will condense from gaseous to solid form with negligible amounts existing in the stratosphere. Thus, H_2 is the only useful opacity source which is known to be distributed uniformly, although its mixing ratio in the atmospheres of Uranus and Neptune is uncertain or unknown.

Part of the data base for Uranus and Neptune in the 8 - 14 μm region is shown in Figure 15. As expected for Uranus, no ν_4 CH_4 or ν_9 C_2H_6 emission features are seen, as they are in the spectra of Jupiter and Saturn. However, the spectrum of Neptune displays emission features of both bands. The existence of CH_4 above an effective cold trap is difficult to understand. Three simple and somewhat distinct explanations

https://doi.org/10.1017/S0074180900075124 Published online by Cambridge University Press

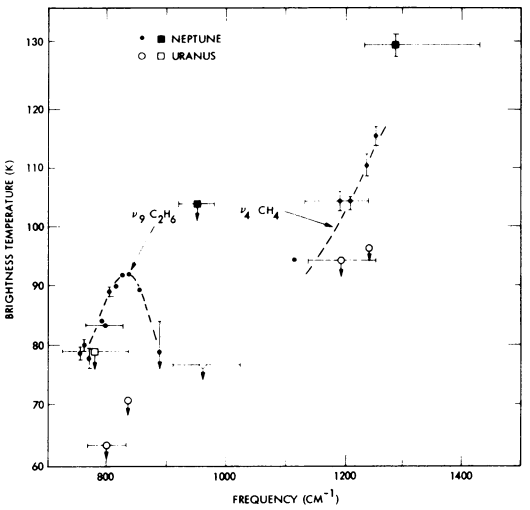

Figure 15. Spectra of Uranus and Neptune for the 8 - 14 μm region (circles from Gillett and Rieke, 1977), squares from Macy and Sinton, 1977). Note the emission features of ethane and methane in the spectrum of Neptune, but not Uranus.

are possible. (A) CH_4 is in saturation equilibrium and strongly depleted in the stratosphere, but is seen because of a very steep temperature inversion supported by aerosol absorption of insolation. (B) CH_4 is in saturation equilibrium below and above the temperature minimum, relatively depleted only near the temperature minimum, although this opens the question as to the origin of the stratospheric CH_4. This model does not require as steep a temperature inversion as model A. (C) CH_4 is uniformly distributed vertically and supersaturated in the stratosphere; presumably this distribution is maintained by a circulation system which acts more rapidly than the time scale for CH_4 freezing. Again, this model does not require as steep a temperature inversion as model A. Why these models (or others) do not appear to operate in the atmosphere of Uranus is unknown, although the answer is probably associated with the peculiar aspect geometry of that planet with respect to the sun and the earth. With the cold south pole facing the earth, all conclusions based on current observational evidence may be characteristic of a colder environment than is true for the global average. The existence of C_2H_6 in the presence of CH_4 is consistent with models of hydrocarbon photochemistry for the outer planets (e.g., Strobel, 1975).

Longer wavelength data for Uranus and for Neptune are displayed in Figures 16 and 17, respectively. Also shown in these figures are spectra resulting from the direct inversion models of Courtin et al. (1978) and Courtin et al. (1979), and the equilibrium models of Appleby and Hogan (1980). The temperature structures corresponding to these models are shown in Figure 18 for Uranus and Neptune. The data are relatively sparse and often broadbanded, attesting to the difficulty of making

https://doi.org/10.1017/S0074180900075124 Published online by Cambridge University Press

observations of these objects in this spectral region. Figures 16 and 17 show that the temperature structure models cannot fit all the available data within quoted errors (although some data in the figures were not considered in the models when published). In addition, the data are occasionally not consistent with each other. Work is clearly called for to remeasure parts of the spectrum, especially with higher spectral resolution where possible.

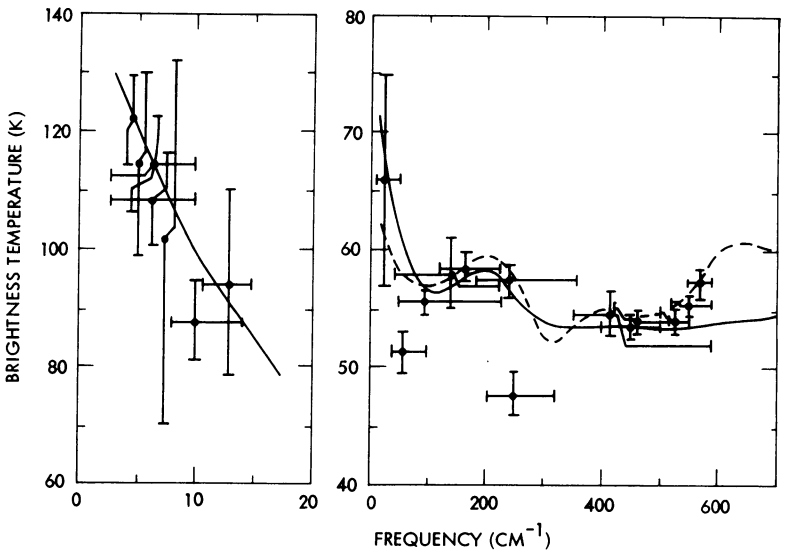

Figure 16. Long wavelength data for Uranus, representing the work of Courtin et al. (1977), Fazio et al. (1976), Gillett (1979), Gillett and Rieke (1977), Hildebrand et al. (1980), Kostenko et al. (1971), Morrison and Cruikshank (1973), Lowenstein et al. (1977a), Rieke and Low (1974), Rowan-Robinson et al. (1978), Stier et al. (1978), Ulich (1974), Ulich and Conklin (1976), Werner et al. (1978) and Whitcomb et al. (1978). Data are plotted at effective spectral positions with FWHM bandpasses (or best estimates where not given explicitly) represented by horizontal bars. No data are shown for frequencies less than 4.5 cm^{-1}. The solid line represents the model spectrum of Courtin et al. (1978) and the dashed line the model spectrum of Appleby and Hogan (1980) (see Fig. 18).

https://doi.org/10.1017/S0074180900075124 Published online by Cambridge University Press

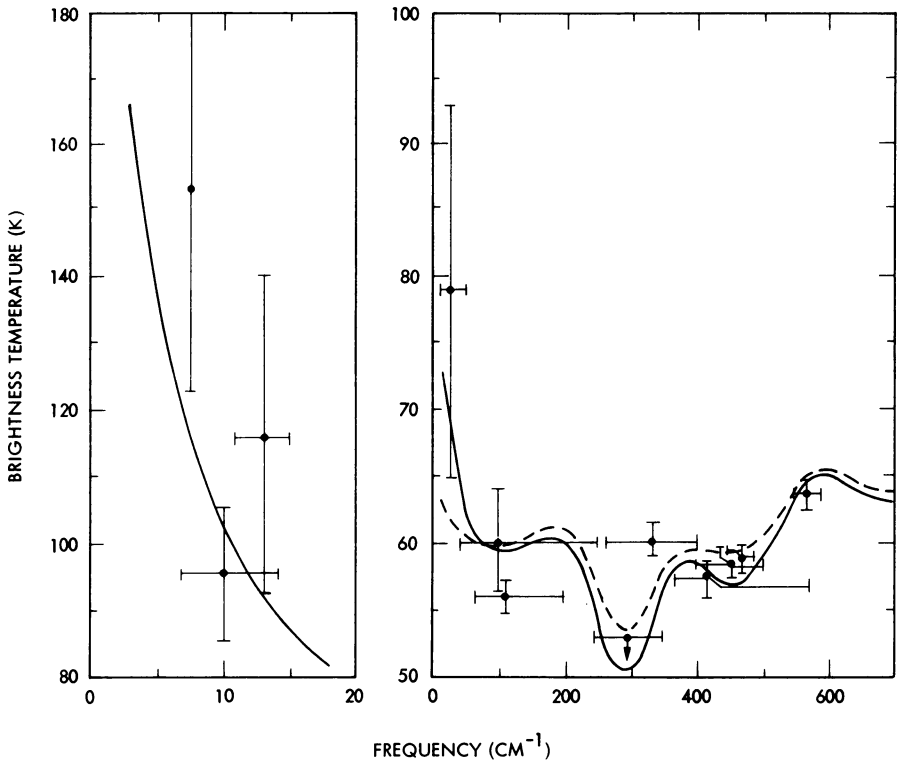

Figure 17. Long wavelength data for Neptune, representing th work of Courtin et al. (1977), Gillett and Rieke (1977), Hild brand et al. (1980), Low et al. (1973), Lowenstein et al. (1977b), Morrison and Cruikshank (1973), Rieke and Low (1974) Steir et al. (1978), Ulich and Conklin (1976), Werner et al. (1978) and Whitcomb et al. (1979). Symbols and spectral ran are the same as for Figure 16. The solid line represents th model spectrum of Courtin et al. (1979) and the dashed line the model spectrum of Appleby and Hogan (1980) (see Fig. 18)

The equilibrium models and direct inversion models are not extremely different from each other (Fig. 18). Differences in the assumed bulk composition for the models shown account for the somewhat different adiabatic lapse rates in the convective region (pressures near or gre than 1 bar). For Uranus, Courtin et al. (1978) assumed an isotherm o lying the highest level sounded in their model I which is shown here (although they did also present results from a model with a hypotheti inverted stratosphere). The shallow thermal inversion in the model c Appleby and Hogan (1980) is a result of insolation absorbed by the existing CH_4 in the stratosphere and a uniform vertical distribution insolation absorbing aerosols. The temperature inversion is, in fac required to match the temperatures deduced by Dunham et al. (1980) f the occultation of SAO158687 by Uranus. For Neptune the models of

https://doi.org/10.1017/S0074180900075124 Published online by Cambridge University Press

Courtin et al. (1979) and Appleby and Hogan (1980) best fitting the data are shown in Fig. 16, chosen from the models for stratospheric CH_4 distribution discussed earlier. Models do not appear to be able to fit all the data well with a "model A type" CH_4 distribution, as discussed above. The Courtin et al. (1979) model corresponds to a "model C type" CH_4 distribution and the Appleby and Hogan (1980) model to a "model B type" distribution.

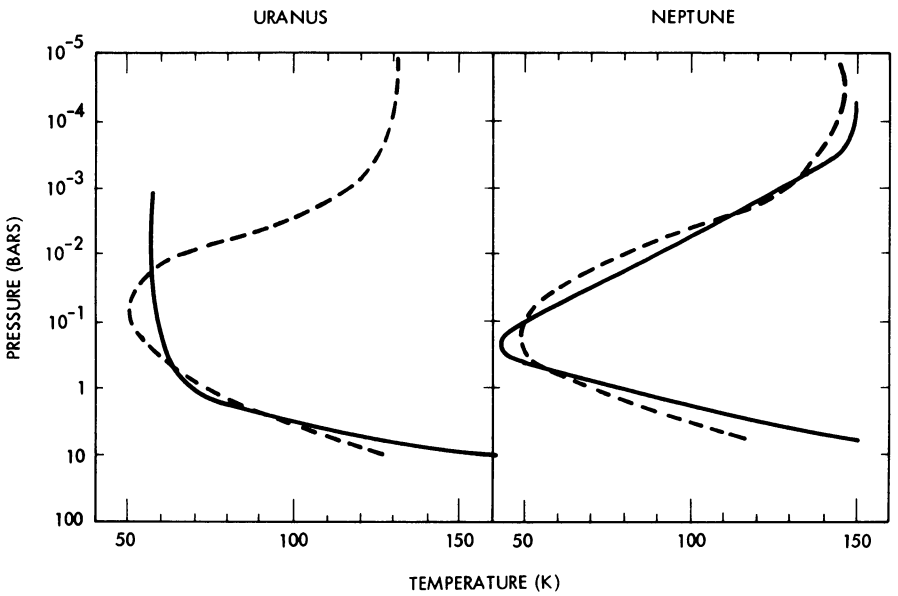

Figure 18. Model temperature structures for Uranus (left) and Neptune (right). Direct inversion models (model I of Courtin et al., 1978) and for Neptune (model N of Courtin et al., 1979) are shown as solid lines. Equilibrium models of Appleby and Hogan (1980) are shown as dashed lines.

Undoubtedly, the models will improve with the addition of better data, ultimately whose spectral resolution will be sufficient to confirm that the collision induced H_2 dipole is, in fact, the dominant opacity. Other substantial improvements in the earth-based data record could result from self-consistent calibration sources from short to long wavelengths. Where broad-band measurements are used in temperature sounding, the full filter response (including telluric extinction) should be convolved with a detailed spectrum, instead of using the monochromatic approximation represented by an effective wavelength or frequency. This would allow a truer calculation of the real weighting function for the filter. As for Jupiter and Saturn, consideration should be given to the possible effect of aerosols (NH_3 and CH_4 ice particles, at least) on the outgoing thermal radiance. Spacecraft experiments to measure thermal flux from Uranus or Neptune with spatial resolution will be difficult due to the low flux levels involved and the associated instrument cooling requirements.

Nevertheless, substantial information is latent in such measurements which can be a key to understanding the climatology and meteorology of these planets, especially for the peculiar insolation conditions of Uranus.

5. CLOSING REMARKS

The most complete kind of planetary information involving high spatial resolution and global coverage can only be provided by spacecraft instrumentation. However, the role of earth-based data and the potential role of infrared observations from earth-orbiting platforms is substantial. Such observations provide the only realistic basis for providing long-term monitoring of time dependent phenomena, and the opportunity for new discovery using spectral regions or resolutions which are, for a variety of reasons, outside the scope of spacecraft experiments.

It is apparent that, even with often very sparse available data, the outer planets demonstrate a remarkable variety of atmospheric properties. Ultimately the results of temperature sounding and energy transport equilibrium models must be combined in order to provide a useful interpretation of the phenomena observed. Future work must address not only the details of the differences among the physical properties of the planets, but underlying reasons and the extent to which they are based on differences of solar distance, obliquity, rotation period and chemical composition.

Acknowledgements are gratefully given to several persons for valuable discussion and support: J. Appleby, J. Bergstralh, J. Caldwell, B. Conrath, D. Gautier, S. Gulkis, R. Hanel, T. Jones, M. Klein, V. Kunde, J. Martonchik, E. Olsen, A. Robiette, and A. Tokunaga; also to D. Gautier and R. Courtin for their earlier review of outer planet thermal structures (1979). This is JPL Atmospheres publication No. 980-13 (internal number) and presents one phase of research carried out at the Jet Propulsion Laboratory, California Institute of Technology, under contract NAS 7-100, sponsored by the Planetary Atmospheres Program Office, Office of Space Science, National Aeronautics and Space Administration.

REFERENCES

APPLEBY, J.F., HOGAN, J., 1980 (in preparation).
ATREYA, S., 1980, communication presented at 23rd Plenary Session of COSPAR, Budapest.
BERGE, G.L., GULKIS, S., 1976, In "Jupiter", T. Gehrels ed., U. of Arizona Press, p. 621.
BIRNBAUM, G., 1978, J. Quant. Spectrosc. Rad. Transf. 19, 51.
CESS, R.D., KHETAN, S., 1973, J. Quant. Spectrosc. Rad. Transf. 13, 995.
CESS, R.D., CHEN, S.C., 1975, Icarus 26, 444.
CHAHINE, M.T., 1972, J. Atmos. Sci. 29, 741.
CHAHINE, M.T., 1975, J. Atmos. Sci. 32, 1946.
CONRATH, B.J., 1972, J. Atmos. Sci. 29, 1262.
CONRATH, B.J., GAUTIER, D., 1980, In "Interpretation of Remotely Sensed Data", A. Deepak ed., Academic Press.

COURTIN, R., CORON, N., ENCRENAZ, T., GISPERT, R., BRUSTON, P., LEBLANC, J., DAMBIER, G., VIDAL-MADJAR, A., 1977, Astron. Astrophys. 60, 115.
COURTIN, R., GAUTIER, D., LACOMBE, A., 1978, Astron. Astrophys. 63, 97.
COURTIN, R., GAUTIER, D., LACOMBE, A., 1979, Icarus 37, 236.
DANIELSON, R.E., 1977, Icarus 30, 462.
DEEPAK, A., 1977, (ed.) "Inversion Methods in Atmospheric Remote Sensing", Academic Press.
DUNHAM, E., ELLIOT, J.L., GIERASCH, P.J., 1980, Astrophys. J. 235, 274.
FAZIO, G.G., TRAUB, W.A., WRIGHT, E.L., LOW, F.J., TRAFTON, L.M., 1976, Astrophys. J. 209, 633.
FLASAR, F.M., CONRATH, B.J., PIRRAGLIA, J.A., CLARK, P.C., FRENCH, R.G., GIERASCH, P.J., 1980, J. Geophys. Res. (in press).
GAUTIER, D., LACOMBE, A., REVAH, I., 1977a, J. Atmos. Sci., 34, 1130
GAUTIER, D., LACOMBE, A., REVAH, I., 1977b, Astron. Astrophys. 61, 149.
GAUTIER, D., MARTEN, A., BALUTEAU, J.P., LACOMBE, A., 1979 Icarus 37, 214.
GAUTIER, D., COURTIN, R., 1979, Icarus 39, 28.
GAUTIER, D., CONRATH, B., FLASAR, M., HANEL, R., KUNDE, J., CHEDIN, A., SCOTT, N., 1980, J. Geophys. Res. (in press).
GILLETT, F.C., RIEKE, G.H., 1977, Astrophys. J 218, L141.
GILLETT, F.C., 1979, unpublished communication.
GULKIS, S., JANSSEN, M.A., OLSEN, E.T., 1978, Icarus 34, 10.
GULKIS, S., OLSEN, E.T., 1980, unpublished communication.
HANEL, R., CONRATH, B., FLASAR, M., KUNDE, V., LOWMAN, P., MAGUIRE, W., PEARL, J., PIRRAGLIA, J., SAMUELSON, R., GAUTIER, D., GIERASCH, P., KUMAR, S., PONNAMPERUMA, C., 1979, Science 204, 972.
HILDEBRAND, R.H., KEENE, J., WHITCOMB, S.E., 1980 (in preparation).
HOGAN, J., RASOOL, I., ENCRENAZ, T., 1969, J. Atmos. Sci. 26, 898.
KLEIN, M.J., JANSSEN, M.A., GULKIS, S., OLSEN, E.T., 1978, In "The Saturn System", NASA Conference Publication CP-2089, p. 195.
KLIORE, A.J., PATEL, I.R., LINDAL, G.F., WAITE, J.H., MCDONOUGH, T.R., 1980, J. Geophys. Res. (in press).
KOSTENKO, V.J., PAVLOV, A.V., SCHOLOMITSKY, G.B., SLYSH, V.I., SOGLASNOVA, V.A., ZABOLOTNY, V.F., 1971, Astrophys. Lett. 8, 41.
LINDAL, G.F., WOOD, G.E., LEVY, G.S., ANDERSON, J.D., SWEETNAM, D.N., HOTZ, H.B. BUCKLES, B.J., HOLMES, D.P., DOMS, P.E., ESHLEMAN, V.R., TYLER, G.L., CROFT, T.A., 1980, J. Geophys. Res. (in press).
LOEWENSTEIN, R.F., HARPER, D.A., MOSELEY, S.H., TELESCO, C.M., THRONSON, H.A., HILDEBRAND, R.H., WHITCOMB, S.E., WINSTON, R., STIENING, R.F., 1977a, Icarus 31, 315.
LOEWENSTEIN, R.F., HARPER, D.A., MOSELEY, H., 1977b, Astrophys. J. 218, L145.
LOW, F.J., RIEKE, G.H., ARMSTRONG, K.R., 1973, Astrophys. J. 183, L105.
MACY, W., SINTON, W.M., 1977, Astrophys. J. 218, L79.
MORRISON, D., CRUIKSHANK, D.P., 1973, Astrophys. J. 179, 329.
OHRING, G., 1973, Astrophys. J. 184, 1027.
OHRING, G., 1975, Astrophys. J. 195, 223.
ORTON, G.S., 1975a, Icarus 26, 125.
ORTON, G.S., 1975b, Icarus 26, 142.

ORTON, G.S., INGERSOLL, A.P., 1976, In "Jupiter", T. Gehrels ed., U. of Arizona Press, p. 206.
ORTON, G.S., 1977, Icarus 32, 41.
ORTON, G.S., ROBIETTE, A.G., 1980, J. Quant. Spectrosc. Rad. Transf. (in press).
ORTON, G.S., INGERSOLL, A.P., 1980, J. Geophys. Res. (in press).
RIEKE, G.H., LOW, F.J., 1974, Astrophys. J. 193, L147.
ROWAN-ROBINSON, M., ADE, P.A.R., ROBSON, E.I., CLEGG, P.E., 1978, Astron. Astrophys. 62, 249.
SINTON, W.M., MACY, W.W., ORTON, G.S., 1980 Icarus 42, 86.
STIER, M.T., TRAUB, W.A., FAZIO, G.G., WRIGHT, E.L., LOW, F.J., 1978, Astrophys. J. 226, 347.
STROBEL, D.F., 1975, Rev. Geophys. Space Phys. 13, 372.
TOKUNAGA, A., CESS, R.D., 1977, Icarus 32, 321.
TOKUNAGA, A.T., CALDWELL, J., GILLETT, F.C., NOLT, I.G., 1978, Icarus 36, 216.
TRAFTON, L.M., 1967, Astrophys. J. 147, 765.
TRAFTON, L.M., STONE, P.H., 1974, Astrophys. J. 188, 649.
ULICH, B.L., 1974, Icarus 21, 254.
ULICH, B.L., CONKLIN, E.K., 1976, Icarus 27, 183.
WALLACE, L., PRATHER, M., BELTON, M.J.S., 1974, Astrophys. J. 193, 481.
WALLACE, L., 1975, Icarus 25, 538.
WALLACE, L., SMITH, G.R., 1976, Astrophys. J. 203, 760.
WERNER, M.W., NEUGEBAUER, G., HOUCK, J.R., HAUSER, M.G., 1978, Icarus 35, 289.
WHITCOMB, S.E., HILDEBRAND, R.H., KEENE, J., STIENING, R.F., HARPER, D.A., 1979, Icarus 38, 75.

DISCUSSION FOLLOWING PAPER DELIVERED BY G. S. ORTON

T. JONES: Occultation data shows a temperature inversion in the atmosphere of Uranus. What can cause the heating?

ORTON: The models derived by Wallace and by Appleby and Hogan have no difficulty in achieving the "warm" temperatures near 10^{-5} bar derived from stellar occultation data. Heating via insolation absorbed by the residual CH_4 above the temperature minimum is sufficient, although stratospheric aerosols may also play an additional role.

WRIGHT: Has He-H_2 collision-induced absorption been measured to 77 K?

ORTON: Yes; the measurements can be found in Figure 6 of Birnbaum (1978, J. Quant. Spectrosc. Rad. Transf. 19, p. 51). Birnbaum has improved these measurements recently, although they are not yet in publication.

WRIGHT: What do you assume for the ortho-para ratio for H_2 in Uranus and Neptune?

ORTON: Equilibrium at the ambient temperature.

WRIGHT: Is there any constituent that could establish equilibrium?

ORTON: We don't know of any. Observations of the H_2 quadrupole absorptions by Smith (1978, Icarus 33, p. 210) tend to indicate equilibrium in Jupiter and Saturn and some evidence for non-equilibrium in Uranus and Neptune.

WRIGHT: There is no translational collision-induced absorption when two J = 0 H_2 molecules collide, so ortho-para equilibrium gives less long wavelength opacity than a 3:1 ortho-para ratio.

ORTON: At this time, an equal or greater source of uncertainty in the infrared absorption is due to the uncertainty in the bulk compositions of Uranus and Neptune.

GULKIS: Your equation of radiative transfer did not include scattering. If scattering is present, how do you differentiate between effects due to thermal structure and effects due to scattering?

ORTON: We cannot differentiate initially between the two effects. We have to look at spectral regions where we think there is evidence for aerosols on some other basis in order to evaluate the scattering. Specific candidates for scatterers can be modeled, for example, but to date we have modeled only a few possible substances.